Ab Initio Molecular Orbital Study of XO_2^+ (X = F, Cl, Br, I) Systems

M. Alcamí, O. Mó,* and M. Yáñez

Departamento de Química, C-9, Universidad Autónoma de Madrid, Cantoblanco, 28049 Madrid, Spain

I. L. Cooper

Department of Chemistry, University of Newcastle upon Tyne, Newcastle upon Tyne, NE1 7RU, United Kingdom

Received: September 24, 1998; In Final Form: February 8, 1999

The structures and relative stabilities of the cationic forms of the halogen dioxides have been studied by means of ab initio molecular orbital calculations. For fluorine- and chlorine-containing compounds the geometries and the harmonic vibrational frequencies of all possible isomers were calculated at the QCISD/6-311+G(2d) level of theory. For bromine- and iodine-containing compounds the effective core-potential basis sets of Hay and Wadt, modified to include a set of diffuse functions and two sets of polarization functions, were employed. For all systems the final energies were obtained at the QCISD(T)/6-311+G(3df) level of theory. In addition, multiconfiguration-based methods (CASSCF and CASPT2) have also been used. The relative stabilities of structures XOO^+ and OXO^+ are greatly reduced relative to those observed for the corresponding neutral species. In fact, for Cl and I derivatives, the lowest energy isomer corresponds to the symmetric OXO^+ open-chain species. The corresponding cyclic structures arise as local minima on the respective potential energy surfaces, but they lie much higher in energy than the OXO^+ open-chain form or the XOO^+ isomer. There are significant differences in bonding between XOO^+ and OXO^+, the X−O interaction in OXO^+ being more covalent than in XOO^+. There are also trends along the series that reflect the pronounced disparity between the electron affinity of F^+ and those of the heavier atoms of the group. FOO^+ species can be viewed as $F(^2P)-O_2^+$ complexes, whereas XOO^+(X = Br, I) species can be regarded as $X^+(^3P)-O_2$ complexes. The OXO^+ open-chain species have an electron charge distribution similar to that of the ozone molecule, reflecting the same number of valence electrons in each case.

Introduction

The depletion of stratospheric ozone has resulted in an increasing interest in the study of the possible reaction mechanisms responsible for its depletion.[1−3] Specifically, particular attention has been devoted recently to the study of reactions involving halogen atoms,[4−8] F, Cl, Br, and I, which may be formed by molecular fragmentation of hydrocarbon−halogen derivatives. In particular, the structure and reactivity of halogen oxides and dioxides has been the subject of a large number of experimental[5−8] and theoretical studies,[9−12] since they may arise as products or intermediates in the reaction cycles for the destruction of ozone by halogens.[2,3] Much less attention has been paid, however, to the corresponding ionic species. In fact there is little information regarding the cationic species where, from a theoretical point of view, only $OClO^+$ [13] and $OBrO^+$ [14] have been studied at a high ab initio level of theory, while experimentally only the IR spectrum of $OClO^+$ has been characterized.[15]

The aim of this paper is to carry out a systematic study of the structures and relative stabilities of the various cationic forms of the halogen dioxides through the use of high level ab initio calculations. One of our goals is to establish whether the ionization of the radical XOO species can produce significant structural rearrangement. It is well established[5−8] that the isomer of lowest energy for all the halogen dioxides is the asymmetric XOO structure rather than the symmetric OXO one. We shall show here that the symmetric forms can be favored when dealing with the corresponding cations. We shall also investigate whether or not the cyclic forms of these species form local minima on the associated potential energy surface (PES) and determine their relative stabilities with respect to the corresponding open-chain forms.

Computational Details

The geometries of the various $[X, O_2]^+$ singlet state cations were optimized at the Quadratic Configuration Interaction level of theory,[16] with inclusion of single and double excitations (QCISD). As we shall discuss in forthcoming sections, approaches based on single determinant wavefunctions may not be appropriate to describe such systems. To this end, we have calculated the so-called T_1 diagnostic, which uses the Euclidean norm of the vector of t_1 amplitudes to assess the reliability of results based on a single reference configuration. A large value of T_1 (>0.02) suggests the need for a multireference procedure.[17,18] For this reason we have also used a Complete Active Space Self-Consistent Field (CASSCF)[19] formalism for the corresponding geometry optimizations. The active space chosen for these CASSCF calculations corresponds to the valence p active space; i.e., it includes twelve electrons distributed over the nine valence p orbitals.

For fluorine- and chlorine-containing species an all-electron 6-311+G(2d)[20] basis set was used in the optimizations. For bromine- and iodine-containing species we have employed the effective core-potential basis sets of Hay and Wadt,[21] modified

10.1021/jp983856n CCC: $18.00 © 1999 American Chemical Society
Published on Web 03/26/1999

to include a set of diffuse sp functions and two sets of d polarization functions.[22] Furthermore, although the valence shell is normally described by a [21] contraction scheme, we have used here a fully uncontracted [111] scheme. When this basis set, denoted hereafter as HW+(2d), is used to describe the halogen atom the oxygen basis set remains the same (6-311+G-(2d)) as that employed in the calculation of F and Cl derivatives.

The corresponding harmonic vibrational frequencies were obtained at the same level of theory as used in the geometry optimizations. This allows the stationary points on the PES to be classified as local minima or saddle points and the corresponding zero point energy (ZPE) corrections to be estimated.

The final energies were obtained in single point calculations at the QCISD(T) level using the 6-311+G(3df)[20,22-24] basis set within the frozen core approximation. Although the geometries of the Br- and I-containing species were optimized using the effective core-potential approach, the final energies were obtained using both the Hay−Wadt basis set augmented with a diffuse sp function and 3df polarization functions[22] (denoted hereafter as HW+(3df)) and an all-electron calculation to permit direct comparison with the corresponding results obtained for F and Cl derivatives. This level of theory corresponds to a G2-type calculation[25] without the use of associated additivity approximations.[26] Hence, the G2(QCI) total energies reported here are obtained by adding to the QCISD(T)/6-311+G(3df) energies the empirical high-level correction defined in ref 26, the unscaled ZPE obtained at the QCISD/6-311+G(2d) level and, in the case of Br and I, the spin−orbit corrections as described in ref 20.

As noted above, the QCISD(T) scheme, based on a single-determinant zero-order wavefunction, may display some serious deficiencies. Therefore the final energies were also obtained using a many-body multireference perturbative treatment[27] (denoted as CASPT2) based on an all-electron 6-311+G(3df) basis set. In these single point calculations the CASSCF optimized geometries were used instead of the QCISD ones. For these CASPT2 calculations we have kept the 1s orbitals of oxygen, fluorine, and chlorine, the 1s2sp orbitals of bromine, and the 1s2sp3spd orbitals of iodine frozen in the perturbational treatment.

Although use of a multireference approach, such as CASSCF/CASPT2, will be shown to remove some of the deficiencies found at the QCISD level, there remain problems inherent in the CASSCF/CASPT2 treatment, such as the appearance of intruder states.[28] In fact, the valence p active space used in our CASSCF/CASPT2 calculations neglects possibly significant excitations[11b,29] to the 3d, 4d, and 5d vacant orbitals of Cl, Br, and I, respectively. A further problem associated with the CASPT2 calculations involves those cases in which the relative energies for species with different numbers of unpaired electrons are computed.[30] As discussed in ref 30, errors of the order of 3 kcal/mol can be obtained, although part of this error can be removed by using the "g3" definition of the zeroth-order Hamiltonian as introduced in the same reference. To test the stability of our CASPT2 results with respect to enlargement of the active space, we have performed for Br and I a series of calculations in which the active space was increased by 1, 2, 3, or 4 orbitals (mainly corrresponding to inclusion of vacant halogen d orbitals). These calculations were used to estimate the singlet−quintet energy gap for $BrOO^+$ and IOO^+. We have also tested the stability of the calculations using the "g3" approach. Results summarized in Table 1 show that for $BrOO^+$ the energy gap is underestimated by 6 kcal/mol when the valence p active space alone is used in the reference wavefunction. The results become stable when three additional vacant orbitals are included in the active space. The use of the "g3" approach systematically generates larger energy gaps, but this correction amounts to only 1.5 kcal/mol. In view of these results, the CASPT2 calculations for the other structures were performed (with the exception of F) with a valence p active space in which three extra d orbitals were included and the "g3" approach used. Due to the computational effort implicit in such enlarged active spaces, geometry and frequency calculations at the CASSCF level were restricted to the valence p active space.

TABLE 1: Stability of the CASPT2 Calculated Singlet−Quintet Energy Gap (kcal/mol) with Respect to an Increasing Number of Orbitals in the Active Space and with Respect to the Use of the "g3" Formulation of the Fock Matrix, as Defined in Ref 30

no. of orbitals (a′, a″)/electrons in the active space	$BrOO^+$ $E(^1A')-E(^5A')$		IOO^+ $E(^1A')-E(^5A')$	
	CASPT2	CASPT2 (g3)	CASPT2	CASPT2 (g3)
(6,3)/12 (valence-p)	−13.4	−17.6	−8.3	−9.8
(7,3)/12	−14.8	−18.4	−8.9	−9.7
(7,4)/12	−19.7	−22.1	−9.5	−10.2
(8,4)/12	−18.9	−21.5	−8.4	−8.9
(8,5)/12	−19.1	−21.4	−8.3	−8.6

The atoms in molecules (AIM) approach of Bader[31] was used to investigate the bonding characteristics of the different species. The bond critical points, i.e., points where the electron density function, $\rho(\mathbf{r})$, is a minimum along the bond path and a maximum along the other two directions, were determined using this formalism. The Laplacian of the electron density, $\nabla^2\rho(\mathbf{r})$, is known[32] to characterize regions of space in which the electronic charge is either locally depleted ($\nabla^2\rho > 0$) or locally enhanced ($\nabla^2\rho < 0$). The former situation is typically associated with interactions between closed-shell systems (ionic bonds, hydrogen bonds, and van der Waals molecules), whereas the latter characterizes covalent bonds, in which the electron density is concentrated in the internuclear region. Exceptions to this general rule are known to exist, particularly when highly electronegative atoms are involved in the bonding, as in the present case. Hence, we have also evaluated the quantity $H(\mathbf{r})$,[33] which does not exhibit such exceptions. In general, negative values of $H(\mathbf{r})$ are associated[33] with a stabilizing charge concentration within the bonding region. However, it should be noted that $H(\mathbf{r})$, defined as the energy density in ref 33, is correctly described as *an* energy density by Bader[31] and is equivalent to the negative of the conventional kinetic energy density $K(\mathbf{r})$. (eq 6.70 in ref 31). For consistency with the earlier literature we shall continue to use the notation $H(\mathbf{r})$ on the understanding that we are considering the negative of the conventional kinetic energy density, $K(\mathbf{r})$.

The AIM analysis was performed using the AIMPAC series of programs[34] modified to calculate contour maps of $H(\mathbf{r})$. All calculations at the QCI level were carried out using the Gaussian-94 series of programs,[35] while geometry and frequency calculations at the CASSCF level have been performed using HONDO-95[36] and CASPT2 energy calculations with the MOLCAS-4[37] program.

Results and Discussion

Structures and Bonding. In principle, three different isomeric arrangements are possible for halogen dioxides. One corresponds to the attachment of the halogen atom to an oxygen atom, while the remaining two are symmetric structures in which the halogen atom occupies the central position and is bonded to both oxygen atoms by forming either a three-membered ring

TABLE 2: T_1 Diagnostic and Total Energies (au) Obtained at Different Levels of Theory for the Compounds Included in This Study[a]

	T_1	QCISD geometry			CASSCF geometry	
	diagnostic	QCISD/6-311+G(2d)[b]	G2(QCI)	G2(QCI-ECP)	CASSCF/6-311+G(2d)[b]	CASPT2 6-311+G(3df)
$FOO^+(^1A')$	0.050	−249.20267 (0.006649)	−249.35838			
$OFO^+(^1A_1)$	0.076					
Cyc-$OFO^+(^1A_1)$	0.028	−249.05358 (0.005488)	−249.20625		−248.58321 (0.005312)	−249.12562
$F(^2P) + O_2(^2\Pi_g)$		−249.21231 (0.004474)	−249.34482		−248.77346 (0.004288)	−249.27474
$F^+(^3P) + O_2(^3\Sigma_g^-)$		−249.02691 (0.003692)	−249.14694		−248.56858 (0.003502)	−249.08358
$ClOO^+(^1A')$	0.056	−609.25913 (0.005607)	−609.42666		−608.84427 (0.005099)	−609.43039
$OClO^+(^1A_1)$	0.027	−609.26708 (0.006364)	−609.45626		−608.82231 (0.005809)	−609.45499
Cyc-$OClO^+(^1A_1)$	0.017	−609.19821 (0.005122)	−609.36846		−608.75392 (0.004585)	−609.35796
$Cl(^2P) + O_2^+(^2\Pi_g)$		−609.24618 (0.004474)	−609.38954		−608.84799 (0.004288)	−609.38999
$Cl^+(^3P) + O_2(^3\Sigma_g^-)$		−609.22835 (0.003692)	−609.35853		−608.78896 (0.003502)	−609.36561
	T_1	QCISD geometry			CASSCF geometry	
	diagnostic	QCISD/HW+(2d)[b]	G2(QCI)	G2(QCI-ECP)	CASSCF/HW+(2d)[b]	CASPT2 6-311+G(3df)
$BrOO^+(^5A')$	0.017	−162.70174 (0.004087)	−2722.26662[d]	−162.84431[d]	−162.27683 (0.003833)	−2722.53471
$BrOO^+(^1A')$	0.063	−162.69287 (0.005292)	−2722.29077	−162.86672	−162.29912 (0.004729)	−2722.56906
$OBrO^+(^1A_1)$	0.034	−162.68962 (0.004912)	−2722.29851	−162.88178	−162.26560 (0.004394)	−2722.56109
Cyc-$OBrO^+(^1A_1)$	0.017	−162.64653 (0.004852)	−2722.24396	−162.82116	−162.22066 (0.004201)	−2722.51114
$Br(^2P) + O_2^+(^2\Pi_g)$		−162.66987 (0.004474)	−2722.24935[d]	−162.82407[d]	−162.28458 (0.004288)	−2722.51224
$Br^+(^3P) + O_2(^3\Sigma_g^-)$		−162.69467 (0.003692)	−2722.25969[d]	−162.83703[d]	−162.27461 (0.003502)	−2722.52759
$IOO^+(^5A')$	0.016	−160.95942 (0.003981)	−7066.88415[d]	−161.11332[d]	−160.55707 (0.003767)	−7066.92624
		−160.95775/−7066.83851[c]				
$IOO^+(^1A')$	0.070	−160.92843 (0.005038)	−7066.87816	−161.10858	−160.56283 (0.004409)	−7066.94037
		−160.91919/−7066.82700[c]				
$OIO^+(^1A_1)$	0.037	−160.94119 (0.004395)	−7066.90276	−161.14141	−160.53149 (0.003859)	−7066.94661
		−160.93240/−7066.85350[c]				
Cyc-$OIO^+(^1A_1)$	0.017	−160.90250 (0.004529)	−7066.85277	−161.08263	−160.49482 (0.004001)	−7066.89214
		−160.90008/−7066.80804[c]				
$I(^2P) + O_2^+(^2\Pi_g)$		−160.88399 (0.004474)	−7066.82220[d]	−161.04980[d]	−160.53413 (0.004288)	−7066.85795
		−160.88218/−7066.77134[c]				
$I^+(^3P) + O_2(^3\Sigma_g^-)$		−160.95407 (0.003692)	−7066.87839[d]	−161.10791[d]	−160.55588 (0.003502)	−7066.91839
		−160.95251/−7066.82979[c]				

[a] For F and Cl complexes QCISD optimizations have been performed by using the 6-311+G(2d) basis set; for Br and I complexes the HW+(2d) basis have been used instead. [b] Values in parentheses correspond to the ZPVE (au) calculated at the same level of theory. [c] First value has been obtained at the CCSD/HW+(2d) level of theory; second one has been obtained at CCSD(T)/6-311+G(3df) level. [d] These values include spin−orbit corrections as quoted in ref 20 (Br = −5.78 mH, Br^+ = −6.77 mH, I = −11.49 mH, I^+ = −13.52 mH). For $XOO^+(^5A')$ structures same spin−orbit correction that for X^+ has been considered.

or an open-chain structure. The total energies of these species at the various levels of theory considered here are given in Table 2, and their relative stabilities with respect to the most stable dissociated form are given in Table 3. The optimized structural parameters are summarized in Table 4.

It can be observed in Table 2 that some of the investigated species present a large value of the T_1 diagnostics, while a few ones present a value reasonably small. As we shall discuss later, for the former there are noticeable discrepancies between calculations based on a single reference configuration and the CASSCF/CASPT2 results. As expected, for the latter, both methodologies yield similar results. Also importantly, we have checked that for all systems which present values of T_1 smaller than 0.02, the dominant configuration weighs at least 85% in the CI expansion, while for systems with large values of T_1 this weight decreases significantly, being in some cases smaller than 50%.

We have to note that the OFO^+ system presents not only a very large value of the T_1 diagnostic (0.076; see Table 2) but also significant inconsistencies between the QCISD and the CASSCF results. At the former level of theory the stationary point found corresponds to an angular arrangement with two imaginary frequencies, while at the latter level the structure found is linear but with an unrealistic electron configuration. Furthermore, at both levels OFO^+ is predicted to be much higher in energy than the FOO^+ isomer, in agreement with the inability of F to dicoordinate. Accordingly, the resulting OFO^+ structure will not be considered in the rest of the discussion.

Some general features can be observed which reflect significant differences in bonding characteristics in moving along the series from F to I. In the case of the XOO^+ species, the O−O distance changes appreciably along the series from F to I. The shortest O−O bond length is found for the fluorine dioxide cation, and this bond length increases when F is replaced successively by Cl and Br and I. In all cases the molecule is predicted to be bent, where the X−O−O bond angle increases on moving from F through to I. These geometrical trends can be understood if one regards these systems as the result of attaching a halogen cation to an oxygen molecule. Since the electron affinity of F^+ is 17.42 eV,[38] attachment to oxygen, with a much lower ionization energy (12.07 eV[39]), yields $F + O_2^+$ through charge transfer. Hence the FOO^+ structure can be viewed as a tightly bound complex formed by the $F(^2P)$ atom and the $O_2^+(^2\Pi_g)$ ion. In fact the positive charge is entirely associated with the O_2 subunit (net charge +0.94e). The two fragments can interact through the unpaired electrons, giving an interaction energy, evaluated at the G2 level, of 8.5 kcal/mol (see Table 3). The Laplacian of the charge density and the values of $H(\mathbf{r})$ within the O−O bond are consistently large and negative, corresponding to a strong covalent linkage. Nevertheless, the value of $\nabla^2\rho(\mathbf{r})$ at the O−F bond critical point is positive but $H(\mathbf{r})$ is negative and smaller in absolute value (see Table 5). Positive values of the Laplacian of the charge density can be found in covalent bonds between two very electronegative atoms,[33] as is the case here. The negative value of $H(\mathbf{r})$ suggests that the interaction has a significant covalent contribu-

TABLE 3: Relative Energies (kcal/mol) for the Different Compounds Included in This Study

	QCISD geometry					CASSCF geometry
	QCISD 6-311+G(2d)	QCISD 6-311+G(3df)	QCISD(T) 6-311+G(3df)	G2(QCI)	G2(QCI-ECP)	CASPT2 6-311+G(3df)
$F(^2P) + O_2^+(^2\Pi_g)$	0.0	0.0	0.0	0.0		0.0[c]
$F^+(^3P) + O_2(^3\Sigma_g^-)$	116.3	118.7	121.6	124.2		119.5[c]
$FOO^+(^1A')$	6.0	3.9	−6.8	−8.5		
Cyc−$OFO^+(^1A_1)$	99.6	97.9	89.4	87.0		94.2[c]
$Cl(^2P) + O_2^+(^2\Pi_g)$	0.0	0.0	0.0	0.0		0.0[c]
$Cl^+(^3P) + O_2(^3\Sigma_{g-})$	11.2	14.2	16.8	19.5		14.8[c]
$ClOO^+(^1A')$	−8.1	−11.4	−20.9	−23.3		−24.8[c]
$OClO^+(^1A_1)$	−13.1	−30.1	−40.0	−41.9		−39.8[c]
Cyc−$OClO^+(^1A_1)$	30.1	23.4	15.9	13.2		20.3[c]

	QSID geometry					CASSCF geometry
	QCISD/ HW+(2d)	QCISD 6-311+G(3df)	QCISD(T) 6-311+G(3df)	G2(QCI)	G2(QCI-ECP)	CASPT2 6-311+G(3df)
$Br(^2P) + O_2^+(^2\Pi_g)$	15.6	11.2	8.5	6.5	8.1	9.6 (10.7)[c,d]
$Br^+(^3P) + O_2(^3\Sigma_g^-)$	0.0	0.0	0.0	0.0	0.0	0.0 (0.0)[c,d]
$BrOO^+(^5A')$	−4.4	−4.4	−4.6	−4.3	−4.6	−4.5 (−4.3)[c,d]
$BrOO^+(^1A')$	1.1	−5.8	−18.6	−19.5	−18.6	−26.0 (−21.0)[c,d]
$OBrO^+(^1A_1)$	3.2	−7.6	−23.2	−24.4	−28.1	−21.0 (−16.2)[c,d]
Cyc−$OBrO^+(^1A_1)$	30.2	21.1	11.9	9.9	10.0	10.3 (14.9)[c,d]
$I(^2P) + O_2^+(^2\Pi_g)$	44.0/44.1[a]	39.1	36.6/36.7[b]	35.3	36.5	37.9 (39.7)[c,d]
$I^+(^3P) + O_2(^3\Sigma_g^-)$	0.0/0.0[a]	0.0	0.0/0.0[b]	0.0	0.0	0.0 (0.0)[c,d]
$IOO^+(^5A')$	−3.4/−3.2[a]	−3.6	−3.8/−5.5[b]	−3.6	−3.4	−4.9 (−4.7)[c,d]
$IOO^+(^1A')$	16.1/20.9[a]	11.1	−3.0/1.8[b]	0.1	−0.4	−13.8 (−4.8)[c,d]
$OIO^+(^1A_1)$	8.1/12.6[a]	−3.0	−18.0/−14.9[b]	−15.3	−21.0	−17.7 (−9.0)[c,d]
Cyc−$OIO^+(^1A_1)$	32.4/32.9[a]	23.3	13.3/13.6[b]	16.1	15.9	16.5 (25.3)[c,d]

[a] Second value has been obtained at the CCSD/HW+(2d) level. [b] Second value has been obtained at the CCSD(T)/6-311+G(3df) level using the CCSD/HW+(2d) geometry. [c] Values including the ZPE correction evaluated at the CASSCF/HW+(2d) level. [d] Values in parentheses include the spin−orbit correction evaluated in the same manner as in the G2 procedure.

TABLE 4: Geometries (Distances in Å, Angles in deg) for the Species Considered in This Study

	R(O−O)		*R*(X−O)		α (deg)	
	QCISD 6-311+G(2d)	CASSC 6-311+G(2d)	QCISD 6-311+G(2d)	CASSCF 6-311+G(2d)	QCISD 6-311+G(2d)	CASSCF 6-311+G(2d)
FOO^+	1.141		1.489		113.7	
Cyc−OFO^+	1.443	1.478	1.504	1.506	57.3	58.7
$ClOO^+$	1.185	1.150	1.788	2.122	118.8	119.8
$OClO^+$			1.428/1.423[b]	1.447	121.0/120.8[b]	121.5
Cyc−$OClO^+$	1.465	1.481	1.710	1.749	50.7	50.8

	R(O−O)		*R*(X−O)		α (deg)	
	QCISD HW+(2d)	CASSCF HW+(2d)	QCISD HW+(2d)	CASSCF HW+(2d)	QCISD HW+(2d)	CASSCF HW+(2d)
$BrOO^+(^5A')$	1.208	1.219	2.771	2.960	176.2	176.5
$BrOO^+(^1A')$	1.198/1.189[a]	1.174	1.918/1.980[a]	2.217	120.0/119.7[a]	121.2
$OBrO^+$			1.603/1.607[c]	1.631	116.7/115.6[c]	116.4
Cyc−$OBrO^+$	1.460	1.511	1.842	1.883	46.7	46.8
$IOO^+(^5A')$	1.208/1.205[a]	1.219	3.063/3.072[a]	3.260	175.2/179.9[a]	176.5
$IOO^+(^1A')$	1.226/1.206[a]	1.209	2.044/2.082[a]	2.597	121.0/121.5[a]	122.1
OIO^+			1.760/1.747[a]	1.794	112.5/112.5[a]	111.7
Cyc−OIO^+	1.462/1.455[a]	1.492	1.982/1.983[a]	2.034	43.3/43.1[a]	43.1

[a] Second value was obtained at the CCSD/HW+(2d) level. [b] Value obtained in ref 13 at the internally contracted MRCI level. [c] Value obtained in ref 14 at the CCSD(T)/6-311G(2df) level.

tion. These bonding characteristics are also reflected in the harmonic frequencies. As illustrated in Table 6, the FO stretching frequency is much lower than that of OO. In relation with FOO^+ it should be also noted that at the CASSCF level FOO^+ dissociates into $F + O_2^+$, in a similar way to what it has been found previously for neutral FOO.[9a]

Charge transfer from the O_2 constituent largely decreases (net charge is +0.53e) when the halogen cation is Cl^+, with an electron affinity of 13.01 eV,[38] which is only 0.94 eV larger than the ionization potential of O_2.[39] The positive charge is now spread over the $ClOO^+$ system. In fact the Cl−O interaction contains an electrostatic contribution as in FOO^+ but the covalent character is enhanced, since Cl can back-donate charge through its d(π) type orbitals. This is reflected in the fact that its predicted dissociation energy into Cl and O_2^+ at the G2 level (23.3 kcal/mol) is three times larger than that estimated for the dissociation of the analogous FOO^+ species, and the O−O distance is also larger than in the corresponding fluorine analog. In FOO^+, the O−O distance is close to that exhibited by the isolated $O_2^+(^2\Pi_g)$ species (1.1227 Å),[39] whereas in $ClOO^+$, where the positive charge of the O_2 constituent is reduced by half, the O−O distance (see Table 4) is intermediate between that of $O_2^+(^2\Pi_g)$ and $O_2(^3\Sigma_g^-)$ (1.207 Å).[39] The situation changes markedly when Cl^+ is replaced by Br^+ or I^+, whose electron

TABLE 5: Bond Characteristics of the Stable Species Included in This Study Calculated Using the QCISD/6-311+G(2d) Density[a]

	OX bond				OO bond			
	ρ	$\nabla^2\rho$	$H(\mathbf{r})$	ϵ	ρ	$\nabla^2\rho$	$H(\mathbf{r})$	ϵ
FOO^+	0.2364	0.5701	−0.1294	0.0514	0.6322	−0.7692	−0.8377	0.0008
Cyc-OFO^+	0.2102	0.5249	−0.1065	0.0144	0.2812	0.1799	−0.1946	0.2056
$ClOO^+$	0.1589	0.1543	−0.0812	0.1003	0.5531	−0.3911	−0.6396	0.0026
$OClO^+$	0.3667	−0.8071	−0.6005	0.1697				
Cyc−$OClO^+$	0.1902	0.0500	−0.1180	0.0215	0.2660	0.2191	−0.1813	0.0867
$BrOO^+(^5A')$	0.0161	0.0670	0.0023	0.1255	0.5129	−0.2858	−0.4053	0.0013
$BrOO^+(^1A')$	0.1215	0.1581	−0.0597	0.1000	0.5329	−0.3113	−0.5926	0.0021
$OBrO^+$	0.2664	0.0940	−0.2897	0.0887				
Cyc−$OBrO^+$	0.1521	0.0958	−0.0886	0.0200	0.2710	0.2042	−0.1860	0.0937
$IOO^+(^5A')$	0.0163	0.0424	0.0014	0.1190	0.5139	−0.2903	−0.5500	0.0009
$IOO^+(^1A')$	0.1134	0.2544	−0.0443	0.0919	0.4899	−0.1657	−0.5041	0.0012
OIO^+	0.2092	0.6482	−0.1649	0.0460				
Cyc−OIO^+	0.1247	0.2858	−0.0602	0.0532	0.2712	0.2061	−0.1850	0.0746

[a] Charge density (ρ), laplacian of the charge density ($\nabla^2\rho$), $H(\mathbf{r}) = -K(\mathbf{r})$ and ellipticity (ϵ). All values in au.

TABLE 6: Unscaled Vibrational Frequencies (cm^{-1}) for All the Species Considered in the Present Study[a]

XOO^+

	QCISD			CASSCF		
	XO stretching	OO stretching	bending	XO stretching	OO stretching	bending
FOO^+	766	1648	504			
$ClOO^+$	638	1440	382	461	1629	147
$BrOO^+(^1A')$	619	1362	342	453	1442	179
$IOO^+(^1A')$	617	1269	326	299	1511	125
$BrOO^+(^5A')$	162	1610	81	77	1547	57
$IOO^+(^5A')$	55	1616	76	51	1546	57

OXO^+

	QCISD			CASSCF		
	sym stretching	asym stretching	bending	sym stretching	asym stretching	bending
$OClO^+$	1012 (1012)[b] 1020 ± 20[c]	1280	500 (511)[b] 520 ± 20[c]	884	1186	480
$OBrO^+$	855 (822)[d]	957 (910)[d]	344 (332)[d]	731	874	323
OIO^+	796	848	284	673	760	259

Cyc−OXO^+

	QCISD			CASSCF		
	OO stretching	OXO asym stretching	OXO sym stretching	OO stretching	OXO asym stretching	OXO sym stretching
Cyc−OFO^+	1024	646	739	956	678	697
Cyc−$OClO^+$	959	687	601	835	617	559
Cyc−$OBrO^+$	940	654	534	801	565	477
Cyc−OIO^+	899	611	477	790	532	434

[a] Values have been obtained with the 6-311+G(2d) basis set for F and Cl and with the ECT+(2d) basis set for Br and I. [b] Value obtained at the internally contrated MRCI level in ref 13. [c] Experimental value taken from ref 15. [d] Value obtained in ref 14 at the CCSD(T) level using the 6-311G(2df) basis set.

affinities (11.84 and 10.45 eV, respectively[38]) are smaller than the ionization potential of O_2. In $BrOO^+$ and IOO^+ species the positive charge is largely associated with the halogen atom (net charges of +0.62e and +0.89e, respectively). Hence, in these cases, the halogen dioxide cation can be viewed as a tightly bound complex between $X^+(^3P)$ and ground state $O_2(^3\Sigma_g^-)$. This is consistent with the fact that the dissociation of $BrOO^+$ into $Br^+ + O_2$ is now energetically more favorable (19.5 kcal/mol) than dissociation into $Br + O_2^+$ (26.0 kcal/mol). Also the O−O distance (see Table 4) in the complex is close to that of isolated $O_2(^3\Sigma_g^-)$ but much larger than that of $O_2^+(^2\Pi_g)$.

Since the molecule is in a singlet spin state, there is an antiferromagnetic coupling between the two triplets on $Br^+(^3P)$ and $O_2(^3\Sigma_g^-)$, and since the alternative ferromagnetic interaction would yield a quintet state, we have investigated the structures and relative stabilities of the quintet species. As shown in Table 4, the X−O distance is much larger in the quintet state cations than in the corresponding singlet state cations. As might be anticipated, the interaction between the halogen cation and the O_2 constituent in these cases is essentially electrostatic, as reflected in a positive value of both $\nabla^2\rho$ and $H(\mathbf{r})$ at the corresponding bond critical point (see Table 5), in a very low value of vibrational stretching frequency (see Table 6), in a practically linear geometrical arrangement (see Table 4), and in the fact that the halogen atom retains a positive charge close to unity (net charge +0.95).

Contour plots of $H(\mathbf{r})$ clearly show the differences in the X−O bond between the singlet and quintet structures. As can be seen in Figure 1, the electronic structure in the vicinity of the halogen atom is not modified in the case of the quintet, but it participates in a covalent bond in the case of the singlet. Similar plots of the Laplacian of the charge density do not reflect so clearly such differences in bond characteristics, since both structures display a positive value of the Laplacian of the charge density, although larger in the case of the quintet.

The OO distance in the IOO^+ molecular ion is also predicted

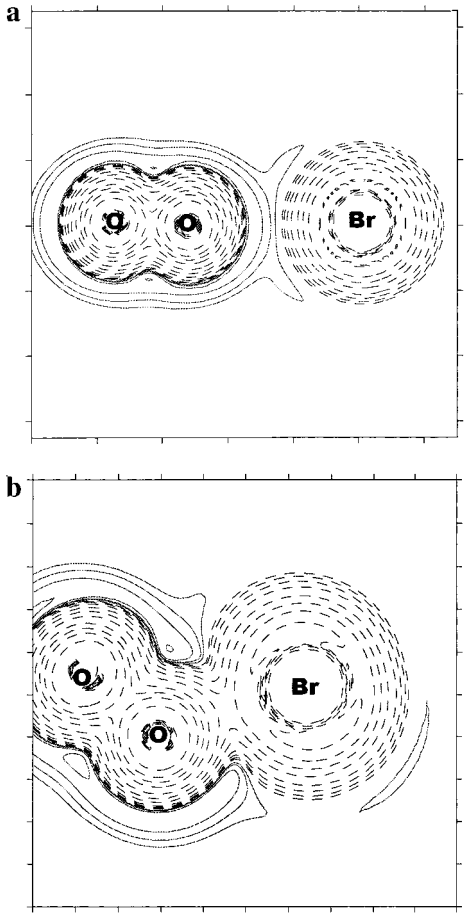

Figure 1. Contour maps of $H(\mathbf{r})$: (a) $BrOO^+(^5A')$; (b) $BrOO^+(^1A')$. Positive values of $H(\mathbf{r})$ are denoted by solid lines and negative values by dashed lines.

to be similar to that of $O_2(^3\Sigma_g^-)$ (1.207 Å) when comparison is made using the CASSCF optimized geometry. However, in contrast to CASSCF, the QCISD optimized geometry predicts an anomalously large value of O−O bond length (1.226 Å; see Table 4), reflecting the inadequacy of the single reference zero-order wavefunction, and consistent with the large value of the T_1 diagnostic for this species (see Table 2). Even though coupled cluster[40] theory including single and double excitations (CCSD) may be considered a more reliable alternative than QCISD for geometry optimizations (the OO distance is predicted to be 1.206 Å; see Table 4), it also presents some problems when relative energies are considered, as will be discussed later.

In OXO^+ systems the halogen atom is covalently bonded to both oxygen atoms. The X−O bond distance is significantly shorter than for the corresponding XOO^+ analogs, and the value of $H(\mathbf{r})$ at the X−O bond critical point is larger in absolute value (see Table 5). The X−O stretching displacements, which appear as symmetric and asymmetric combinations, have consistently higher frequencies than the X−O stretch in the analogous XOO^+ species (see Table 6). This covalent character is especially marked in the case of $OClO^+$, the only isomer that simultaneously displays large negative values of the Laplacian of the charge density and the energy density. All OXO^+ open chain species possess an electronic charge distribution rather similar to that of ozone, with an equivalent number of valence electrons. Thus, although these species correspond to an overall singlet multiplicity, both oxygen atoms possess significant radical character, arising from a non-negligible contribution from configurations which involve the HOMO−LUMO excitation.

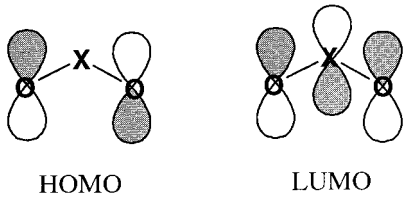

HOMO LUMO

In fact, our results show that the weight of these configurations and the natural orbital populations in our CASSCF treatment for the particular case of the $OBrO^+$ and OIO^+ species are almost equal to those found at the same level of treatment for ozone.

The cyclic OXO^+ species are characterized by rather similar O−O bond distances, typical of an O−O single bond. The oxygen−halogen distances and charge densities show that the interaction is significantly weaker than that in the open chain structures but is still larger than that in XOO^+ systems (see Tables 4 and 5). All four cyclic species were found to be local minima of the PES, which is not the case for the corresponding neutral species. In addition, the electronic charge distributions of these cyclic species closely resemble that of the trioxirane, i.e., the O_3 system with D_{3h} symmetry, with an equivalent number of valence electrons. Hence, it is not surprising to find that, just as trioxirane is estimated to be[41] 29.3−32.2 kcal/mol higher in energy than ozone, the OXO^+ cyclic species lie higher in energy than the open-chain analogs (by 34.3 kcal/mol for Br, by 31.4 kcal/mol for I, and by 55.1 kcal/mol for Cl).

Relative Stabilities. Table 3 summarizes the energies of the different $[X, O_2]^+$ halogen dioxide cations with respect to the lower of the $X + O_2^+$ and $X^+ + O_2$ dissociation limits. From the values in Table 3 it is apparent that the calculated relative energies are quite sensitive both to the quality of the basis set and to the level of theory employed. For instance, the FOO^+ species is predicted to be unstable with respect to dissociation into $F + O_2^+$ at the QCISD/6-311+G(2d) level of theory. This unphysical result remains when the larger 6-311+G(3df) basis set is used. Only when the triple excitations are taken into account, in a QCISD(T) calculation using the largest basis set, is a more realistic result obtained, which predicts FOO^+ to lie 6.8 kcal/mol below its dissociation limit. The importance of triple excitations is also apparent in the chlorine system: although $ClOO^+$ is predicted to lie below its dissociation limit at the QCISD level of theory, the inclusion of triple excitations provides a stabilization of 9.5 kcal/mol. This effect is even more pronounced in the bromine and iodine containing compounds.

These results point to a serious deficiency in the ability of the QCISD formalism to describe the energetics of such systems. This is confirmed when comparing the relative energies of the XOO^+ (X = Br, I) cations in singlet and quintet states, since the quintets are incorrectly predicted to lie lower in energy than the singlets. This situation, in the particular case of bromine-containing compounds, appears to have been resolved when triple excitations are included in the theoretical treatment. However, the problem still remains, even at the G2 level, for iodine-containing systems. It can be seen from Table 3 that CCSD and CCSD(T) results lead to similar or even poorer energy predictions. This problem disappears when the zero-order wavefunction is no longer a single determinant, as in the CASPT2 formalism. At this level the singlet is always predicted to lie below the quintet (see Table 1), the best estimate for the energy gap being 8.9 kcal/mol. Nevertheless, the energy gap between singlets and quintets decreases significantly when spin−orbit coupling is taken into account. These effects, which in first order vanish for the singlet, are of the order of 8.5 kcal/

mol for the quintet, assuming the same value of spin−orbit coupling as in $I^+(^3P)$.[22] As a consequence, singlet and quintet IOO^+ states should be nearly degenerate in energy.

With the exception of fluorine derivatives, where F is not able to form dicoordinated structures, the open-chain OXO^+ species are largely stabilized with respect to XOO^+ when compared with the corresponding neutral species. In the case of chlorine derivatives, neutral ClOO is known[6,10a] to lie lower in energy than OClO by 1.6 kcal/mol, while $OClO^+$ is predicted to lie lower in energy than $ClOO^+$ by 18.6 kcal/mol. In the case of bromine derivatives, BrOO has been estimated to lie 10.9 kcal/mol lower in energy than OBrO[7,11b] while a CASPT2 calculation on the cations predicts a reduction of the energy gap to 4.8 kcal/mol. In contrast, at the G2(QCI) level the $OBrO^+$ structure is predicted to be 4.9 kcal/mol below the $BrOO^+$ species.

For iodine derivatives, the relative stability of the two structures is reversed, in the sense that neutral IOO is estimated to be 10.5 kcal/mol lower in energy[8] that OIO, whereas for the cations CASPT2 predicts OIO^+ to lie 4.2 kcal/mol below IOO^+. These changes for the cationic species relative to those of the corresponding neutral species indicate that the ionization process preferentially stabilizes the symmetric isomer, the ionization potentials of the symmetric OXO structures being significantly lower than those of the asymmetric XOO structures. For instance, comparing with the results at the G2(QCI) level reported in ref 11b, we can evaluate the ionization potentials of BrOO and OBrO to be 251.9 and 237.2 kcal/mol, respectively, in good agreement with the recently reported value[14] of 234.4 kcal/mol for OBrO.

This can be understood by examining the characteristics of the highest singly-occupied molecular orbital of the neutral species. For XOO systems, the HOMO is dominated by the oxygen lone pair. Strictly speaking,

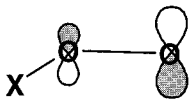

it has an antibonding character with respect to the oxygen atoms, but with a large contribution from the atomic orbitals of the terminal oxygen, while there is no contribution from the atomic orbitals of the halogen atom. The HOMO of the symmetric OXO isomer is antibonding with respect to the halogen and both oxygen atoms and therefore lies higher in energy. Consistently, the effect of ionization is to strengthen the O−O bond in XOO^+ species, while both O−X bonds are strengthened in OXO^+ structures.

We note that the energy gap between XOO^+ and OXO^+ is clearly larger for Cl (18.6 kcal/mol) than for Br (+4.9 or −4.8 kcal/mol depending upon the level of theory considered) and I (4.2 kcal/mol). This result can be viewed as a direct consequence of the relative stability of the X−O bonds. In fact, on going from XOO^+ to OXO^+ structures, an O−O bond essentially is replaced by an X−O bond. Hence the relative stability of the OXO^+ systems should be governed by the relative stability of the X−O bond. It is reasonable to expect the relative stabilities of OXO^+ structures to follow the same trend, Cl ≫ Br ≈ I, as the experimental dissociation energies of the corresponding XO monoxides (the experimental dissociation energies for ClO, BrO, and IO are 64.2,[42] 55.3,[7] and 54.0,[8] respectively). The higher stability of the ClO bonds in $OClO^+$ is clearly reflected in the analysis of the charge density, as pointed out above.

The OXO^+ cyclic structures are the highest energy ones, although they all constitute local minima on the corresponding PES, and we note from Table 5 that the relative stability of these forms increases along the series. While the gap between FOO^+ and the cyclic OFO^+ isomer is 95.5 kcal/mol, that between $BrOO^+$ and the cyclic $OBrO^+$ isomer is only 29.4 kcal/mol. However, even in this latter case the cyclic form lies above the $Br^+ + O_2$ dissociation limit.

Conclusions

From our ab initio calculations we conclude that OXO^+ structures are stabilized with respect to those of XOO^+, when compared with the corresponding neutral species. For Cl and I the OXO^+ structure lies lower in energy than XOO^+, in contrast with the situation for the neutrals. In the case of Br the relative stabilities of $OBrO^+$ and $BrOO^+$ isomers depend on whether multireference based or single-reference based methods are employed. Taking into account that for both structures a considerably high value of the T_1 diagnostic was found, one should consider the CASPT2 estimates more reliable. Nevertheless, both methods agree in predicting a large reduction in the BrOO−OBrO energy gap in going from the neutral to the cation. This implies that the ionization of the halogen dioxides preferentially stabilizes the symmetric OXO structures because both O−X bonds become strengthened. The corresponding cyclic structures occur as local minima on the relevant potential energy surfaces, but they lie much higher in energy than the open-chain OXO^+ or XOO^+ isomers. Significant differences in bonding occur between the XOO^+ and OXO^+ structures, the X−O interaction in OXO^+ having a higher covalent character. This implies significant differences in bonding along the series, reflecting the significant difference between the electron affinity of F^+ and those of the heavier atoms of the group. The FOO^+ species can be viewed as an $F(^2P)-O_2^+(^2\Pi_g)$ complex, while the XOO^+ (X = Br, I) species can be viewed as $X^+(^3P)-O_2(^3\Sigma^-_g)$ complexes. We have also found that the antiferromagnetic interaction of both triplet subunits within an overall singlet multiplicity gives a lower energy than the corresponding ferromagnetic interaction within an overall quintet multiplicity. This arises because the interaction between the subunits in the latter can only be electrostatic, whereas covalent contributions are permitted in the former.

In addition, the OXO^+ open-chain species have an electronic charge distribution similar to that exhibited by the ozone molecule, with an equivalent number of valence electrons, implying that the two oxygen atoms possess a certain radical character, despite having an even number of electrons.

Acknowledgment. This work has been partially supported by the DGES Project No. PB96-0067 and NATO collaborative reseach grant No. 951276. A generous allocation of computing time at the "Centro de Computacion Científica de la Facultad de Ciencias" at the Universidad Autonoma de Madrid is also acknowledged.

References and Notes

(1) Rowland, F. S. *Annu. Rev. Phys. Chem* **1991**, *42*, 731.
(2) (a) Molina, M. J.; Rowland, F. S. *Nature* **1974**, *249*, 819. (b) Molina, L. T.; Molina, M. J. *J. Chem. Phys.* **1987**, *91*, 433.
(3) (a) McElroy, M. B.; Salawitch, R. J.; Wofsy, S. C.; Logan, J. A. *Nature* **1986**, *321*, 759. (b) Brune, W. H.; Anderson, J. G.; Toohey, D. W.; Fahey, D. W.; Kawa, S. R.; Jones, R. L.; McKeena, D. S.; Poole, L. R. *Science* **1991**, *252*, 1261.
(4) Wayne, R. P.; Poulet, G.; Biggs, P.; Burrows, J. P.; Cox, R. A.; Crutzen, P. J.; Hayman, G. D.; Jenkin, M. E.; Le Bras, G.; Moortgat, G. K.; Platt, U.; Schindler, R. N. *Atmos. Environ.* **1995**, *29*, 2677.
(5) Chase, M. W. *J. Phys. Chem. Ref. Data* **1996**, *25*, 551.
(6) Abramowitz, S.; Chase, M. W. *Pure Appl. Chem.* **1991**, *63*, 1449.
(7) Chase, M. W. *J. Phys. Chem. Ref. Data* **1996**, *25*, 1069.

(8) Chase, M. W. *J. Phys. Chem Ref. Data* **1996**, *25*, 1297.

(9) (a) Francisco, J. S; Zhao, Y.; Lester, W. A., Jr.; Williams, I. H. *J. Chem. Phys.* **1992**, *96*, 2861. (b) Ventura, O. N.; Kieninger, M. *Chem. Phys. Lett.* **1995**, *245*, 488. (c) Kieninger, M.; Segovia, M.; Ventura, O. N. *Chem. Phys. Lett.* **1998**, *287*, 597.

(10) (a) Peterson, K. A.; Werner, H. J. *J. Chem. Phys.* **1992**, *96*, 8948. (b) Peterson, K. A.; Werner, H. J. *J. Chem. Phys.* **1996**, *105*, 9823.

(11) (a) Pacios, L. F.; Gómez, P. C. *J. Phys. Chem. A* **1997**, *101*, 1767. (b) Alcami, M.; Cooper, I. L. *J. Chem. Phys.* **1998**, *108*, 9414. (c) Workman, M. A.; Francisco, J. S. *Chem. Phys. Lett.* **1998**, *293*, 65.

(12) Misra, A.; Marshall, P. *J. Phys. Chem. A* **1998**, *102*, 9056.

(13) Peterson, K. A.; Werner, H. J. *J. Chem. Phys.* **1993**, *99*, 302.

(14) Francisco, J. S. *Chem. Phys. Lett.* **1998**, *288*, 307.

(15) Flesch, R.; Rühl, E.; Hottmann, K.; Baumgärtel, H. *J. Phys. Chem. A* **1993**, *97*, 837.

(16) Pople, J. A.; Head-Gordon, M.; Raghavachari, K. *J. Chem. Phys.* **1987**, *87*, 5968.

(17) Lee, T. J.; Rice, J. E.; Scuseria, G. E.; Schaefer, H. F. *Theor. Chim. Acta* **1989**, *75*, 81.

(18) Lee, T. J.; Taylor, P. R. *Int. J. Quantum. Chem. Symp.* **1989**, *23*, 199.

(19) (a) Roos, B. J. *Adv. Chem. Phys.* **1987**, *69*, 399. (b) Shepard, R. *Adv. Chem. Phys.* **1987**, *69* and references therein.

(20) (a) Krishan, R.; Binkley, J. S.; Seeger, R.; Pople, J. A. *J. Chem. Phys.* **1980**, *72*, 650. (b) McLean, A. D.; Chandler, G. S. *J. Chem. Phys.* **1980**, *72*, 5639.

(21) Hay, P. J.; Wadt, W. R. *J. Chem. Phys.* **1985**, *82*, 284.

(22) Glukhovtsev, M. N.; Pross, A.; McGrath, M. P.; Radom, L. *J. Chem. Phys.* **1995**, *103*, 1878.

(23) McGrath, M. P.; Radom, L. *J. Chem. Phys.* **1991**, *94*, 511.

(24) Curtiss, L. A.; McGrath, M. P.; Blaudeau, J. P.; Davis, N. E.; Binning, R. C., Jr.; Radom, L. *J. Chem. Phys.* **1995**, *103*, 6104.

(25) Curtiss, L. A.; Raghavachari, K.; Trucks, G. W.; Pople, J. A. *J. Chem. Phys.* **1991**, *94*, 7221.

(26) Curtiss, L. A.; Carpenter, J. E.; Raghavachari, K.; Pople, J. A. *J. Chem. Phys.* **1992**, *96*, 9030.

(27) Andersson, K.; Ross, B. O. In *Modern Electronic Structure Theory Part II*; Yarkony, D. R., Ed.; World Scientific: Singapore, 1995.

(28) Ross, B. O.; Andersson, K.; Fulscher, M. P.; Malmqvist, P.; Serrano-Andres, L.; Pierloot, K.; Merchán, M. *Adv. Chem. Phys.* **1996**, *93*, 219.

(29) Pettersson, L. G. M.; Siegbahn, P. E. M. *J. Chem. Phys.* **1985**, *83*, 3538.

(30) Andersson, K. *Theor. Chim. Acta* **1995**, *91*, 31.

(31) Bader, R. F. W. *Atoms in Molecules. A Quantum Theory*; Oxford University Press: New York, 1990.

(32) (a) Bader, R. F. W.; Essén, H. *J. Chem. Phys.* **1984**, *80*, 1943. (b) Bader, R. F. W.; MacDougall, P. J.; Lau, C. D. H. *J. Am. Chem. Soc.* **1984**, *106*, 1594. (c) Wiberg, K. B.; Bader, R. F. W.; Lau, C. D. H. *J. Am. Chem. Soc.* **1987**, *109*, 985.

(33) Cremer, D.; Kraka, E. *Angew. Chem. Int. Ed. Engl.* **1984**, *23*, 627.

(34) The AIMPAC programs package has been provided by J. Cheeseman and R. F. W. Bader.

(35) Gaussian 94. Frisch, M. J.; Trucks, G. W.; Schlegel, H. B.; Gill, P. M. W.; Johnson, B. G.; Robb, M. A.; Cheeseman, J. R.; Keith, T. A.; Peterson, G. A.; Montgomery, J. A.; Raghavachari, K.; Al-Laham, M. A.; Zakrzewski, V. G.; Ortiz, J. V.; Foresman, J. B.; Cioslowski, J.; Stefanow, B. B.; Nanayaklara, A.; Challacombe, M.; Peng, C. Y.; Ayala, P. Y.; Chen, W.; Wong, M. W.; Andres, J. L.; Replogle, E. S.; Gomperts, R.; Martin, R. L.; Fox, D. J.; Binkley, J. S.; Defrees, D. J.; Baker, J.; Stewart, J. P.; Head-Gordon, M.; Gonzalez, C.; Pople, J. A. Gaussian, Inc.: Pittsburgh, PA, 1995.

(36) Dupuis, M.; Marquez, A.; Davidson, E. R. *HONDO-95 from CHEM-Station*; IBM Corp.: Kingston, 1995.

(37) MOLCAS Version 4. Andersson, K.; Blomberg, M. R. A.; Fulscher, M. P.; Kalstrom, G.; Lindh, R.; Malmqvist, P. A.; Neogrady, P.; Olsen, J.; Roos, B. O.; Sadlej, A. J.; Schutz, M.; Seijo, L.; Serrano-Andres, L.; Siegbahn, P. E. M.; Widmark, P. O. University of Lund, Sweden, 1997.

(38) Moore, C. E. *Atomic Energy Levels Vol. I, II, and III*; National Bureau of Standards: Washington, DC, 1971.

(39) Huber, K.; Herzberg, G. *Molecular Spectra and Molecular Structure 4. Constants for diatomic molecules*; Van Nostrand: Princeton, NJ, 1979.

(40) (a) Cizek, J. *Adv. Chem. Phys.* **1969**, *14*, 34. (b) Purvis, G. D.; Bartlett, R. J. *J. Chem. Phys.* **1982**, *76*, 1910.

(41) Müller, T.; Xantheas, S. S.; Dachsel, H.; Harrison, R. J.; Nieplocha, J.; Shepard, R.; Kedziora, G. S.; Lischa, H. *Chem. Phys. Lett.* **1998**, *293*, 72.

(42) Atkinson, R.; Baulch, D. L.; Cox, R. A.; Hampson, R.F., Jr.; Kerr, J. A.; Rossi, M. J.; Troe, J. *J. Phys. Chem. Ref. Data* **1997**, *26*, 1329.